Bistability in a stochastic RNA-mediated gene network

Jason Lloyd-Price and Andre S. Ribeiro*
Laboratory of Biosystem Dynamics, Department of Signal Processing, Tampere University of Technology, P.O. Box 527, FI-33101 Tampere, Finland

(Received 3 May 2013; revised manuscript received 10 July 2013; published 23 September 2013)

Small regulatory RNAs (srRNAs) are important regulators of gene expression in eukaryotes and prokaryotes. A common motif containing srRNA is a bistable two-gene motif where one gene codes for a transcription factor (TF) which represses the transcription of the second gene, whose transcript is a srRNA which targets the first gene's transcript. Here, we investigate the properties of this motif in a stochastic model which takes the low copy numbers of the RNA components into account. First, we examine the conditions for stability of the two "noisy attractors." We find that for realistic low copy numbers, extreme, but within realistic intervals, mutual repression strengths are required to compensate for the variability of the RNA numbers and thus, achieve long-term bistability. Second, the promoter initiation kinetics is found to strongly influence the bistability of the switch. Super-Poissonian RNA production disrupts the ability of the srRNA to silence its target, though sub-Poissonian RNA production does not rule out the need for strong mutual repression. Finally, we show that asymmetry between the two interactions forming the switch allows an external input to induce the transition from "high srRNA" to "'high TF" more easily (i.e., with a shorter input) than in the opposite direction. We hypothesize that this asymmetric switching property allows these circuits to be more sensitive to one external input, without sacrificing the stability of one of the noisy attractors.

DOI: 10.1103/PhysRevE.88.032714 PACS number(s): 87.18.Cf, 87.18.Tt, 87.10.Mn, 87.14.gn

I. INTRODUCTION

Small noncoding regulatory RNAs (srRNAs) have been found targeting the majority of eukaryotic genomes [1], and are abundant in prokaryotes as well [2,3]. In bacteria, srRNAs generally modify the expression of their target genes by binding to the 5′ region of the messenger RNA, and inhibit translation by blocking the ribosome binding site [3], usually resulting in the degradation of the target mRNA and often also the srRNA [3]. This regulation scheme differs from transcription factor (TF) based regulation in several aspects, the most important being that when the target is expressed at a lower rate than the srRNA, it is nearly fully silenced [4], while above the srRNA production rate, the target's expression increases linearly. This regulatory function is highly nonlinear and is believed to be responsible for several complex behaviors in genetic circuits [5].

TF-based and srRNA-based regulatory mechanisms function together in gene regulatory networks, and a number of such mixed motifs have been identified including various feedforward and feedback loops [6]. Of interest is the srRNA-mediated double feedback loop (SMDFL), which is present in both eukaryotic and prokaryotic organisms (see, for example, [6–12]). In this motif, a srRNA represses a gene, whose protein is a TF which represses transcription of the srRNA. This network has been shown to exhibit bistability [7], and can thus operate as a switch, similar to the genetic Toggle Switch motif in which two TFs mutually repress each other [13].

Some bistable circuits are involved in cell fate decisions [14,15], including the SMDFL [9–12]. Such switches must remain in a state for long periods of time [16]. On the other hand, cell populations can take advantage of unstable switches to generate phenotypic diversity and increase fitness in unpredictable environments [17]. One source of instability is noise in gene expression.

srRNA-mediated repressive interactions have interesting noise properties [4]. When the srRNA production rate is significantly below the target mRNA production rate, the noise in the protein numbers over time, as measured by the Fano factor, is as in the unrepressed system. On the other hand, when the srRNA production rate is significantly above the production rate of the target mRNA, the protein Fano factor decreases to 1, since the srRNA decreases the protein burst size from each mRNA and, consequently, protein production becomes Poissonian [4]. When the two rates are approximately equal, near-critical phenomena increase the noise in the protein numbers beyond the level in the nonrepressed case [18]. This noise is, in turn, dependent on the initiation kinetics at the promoter, for which evidence exists for a range of kinetics, from bursty [19,20], to sub-Poissonian [21,22]. Given the above, it is nonobvious how low RNA copy numbers affect the dynamics of the SMDFL.

Here, we study the behavior of a stochastic model of the SMDFL within realistic parameter ranges. We focus on how the behavior of the switch is affected by low copy numbers, TF repression strengths, srRNA production rates, and different promoter initiation kinetics. Finally, we study how asymmetries between the two interactions forming the switch affect its sensitivity to external inputs.

II. METHODS

A. Stochastic model of the srRNA-mediated double feedback loop

We use a stochastic version of the srRNA-mediated double feedback loop model presented in [7]. This model, depicted in

*Author to whom correspondence should be addressed: andre.ribeiro@tut.fi

 ©2013 American Physical Society

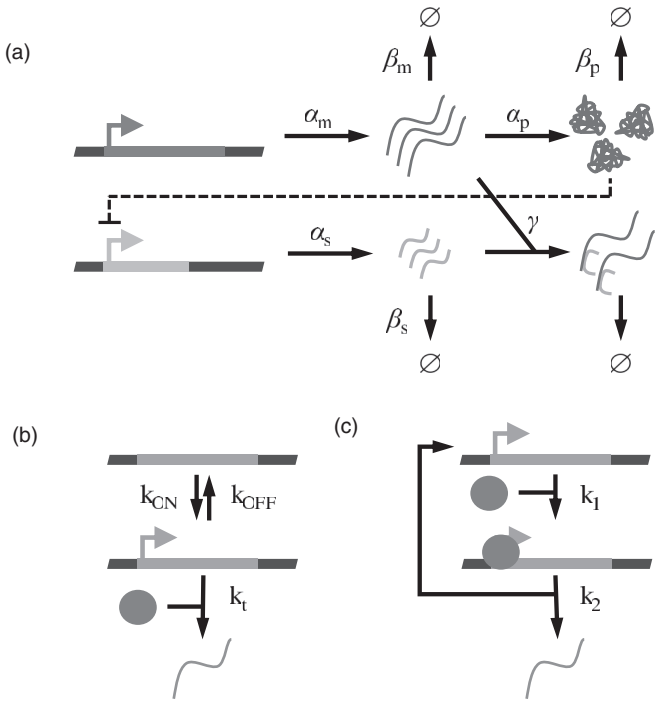

FIG. 1. Cartoon of the model. (a) mRNA (dark gray) and srRNA (light gray) are transcribed from the DNA with mean rates α_m and α_s, respectively, degrade via first-order reactions with rates β_m and β_s, respectively, and irreversibly bind to one another with rate γ. The mRNA is translated into transcription factors with mean rate α_p, which degrade as a first-order reaction with rate β_p, and can bind to the srRNA gene's promoter, repressing it. (b) Telegraph model of transcription regulation [19]. The gene stochastically switches between OFF and ON states. RNA polymerase (ball) can transcribe the gene only when it is ON. (c) Multistep model of transcription initiation [25]. The RNA polymerase (ball) must perform a series of time-consuming steps (here two) to initiate transcription. The parameters are explained in Table I.

Fig. 1(a), consists of reactions (1)–(9):

$$\mathrm{Pro}_m \xrightarrow{\alpha_m} \mathrm{Pro}_m + R_m, \quad (1)$$

$$R_m \xrightarrow{\beta_m} \emptyset, \quad (2)$$

$$R_m \xrightarrow{\alpha_p} R_m + P, \quad (3)$$

$$P \xrightarrow{\beta_p} \emptyset, \quad (4)$$

$$\mathrm{Pro}_s \xrightarrow{\alpha_s} \mathrm{Pro}_s + R_s, \quad (5)$$

$$R_s \xrightarrow{\beta_s} \emptyset, \quad (6)$$

$$R_m + R_s \xrightarrow{\gamma} \emptyset, \quad (7)$$

$$\mathrm{Pro}_s + P \xrightarrow{k_r} \mathrm{Pro}_s \bullet P, \quad (8)$$

$$\mathrm{Pro}_s \bullet P \xrightarrow{k_u} \mathrm{Pro}_s + P. \quad (9)$$

Here, m and s are the genes producing the TF and the srRNA, respectively. Pro_x and R_x are the promoter of gene x and its transcript, respectively. P is the TF and $\mathrm{Pro}_s \bullet P$ is the repressed promoter.

It is worth mentioning that srRNA regulation is achieved in a number of ways. Firstly, srRNA can bind to the target and actively promote degradation of both the target and regulatory RNAs [reaction (7)]. Alternatively, the srRNA may bind to the target and prevent translation, but not promote degradation. If this binding is strong and the srRNA cannot dissociate from the mRNA, this is dynamically equivalent to the first scenario since, in both cases, the mRNA is unable to produce proteins after the srRNA-mRNA binding event. The weak-binding scenario is not considered here, due to its requiring modifications in the model that are beyond the scope of this work. A third option exists, also not considered here for similar reasons, whereby the srRNA promotes the degradation of the target, but is not itself consumed [23].

Most parameters of the model were set to realistic values (Table I). The remaining ones were reparametrized to introduce three dynamically relevant, but not necessarily physically relevant parameters: θ, R, and λ. θ controls the system size, which scales the mean copy numbers of RNA and proteins in the model, and was arbitrarily chosen to represent the mean number of mRNA molecules if there were no srRNA regulation (specifically, $\alpha_m = \theta\beta_m$). Decreasing θ increases low-copy-number effects, while increasing θ makes the system more similar in behavior to the deterministic solution (see Supplemental Material [24]). R controls the strength of the TF's repression of the srRNA gene's promoter by setting the dissociation constant TF-promoter interactions to $\mu_P R^{-1}$, where μ_P is the mean amount of TF produced with no srRNA interaction (specifically, $K_d = \mu_P R^{-1} = \alpha_m B \beta_p^{-1} R^{-1}$). Thus, a value of 2 sets K_d to one half of the unrepressed TF mean. Lastly, λ controls the srRNA repression efficiency, and is equal to the ratio between srRNA production and mRNA production, in the absence of TF regulation (specifically, $\alpha_s = \lambda\alpha_m$). Higher λ increases the repression strength of the srRNA. λ must be at least 1 in order to fully silence the gene. Note that since α_s is a multiple of α_m, the mean srRNA production rate also scales with θ.

In this model, only a single TF represses the srRNA promoter [reactions (8) and (9)]. Since it does so as a monomer, the repression does not introduce nonlinear effects. Nonlinear mechanisms, such as cooperativity and multimerization, can greatly enhance the stability of a switch, though they are not necessary [25]. If bistability is observed in the present model, it should also be observable and enhanced in a model with these properties [25]. We therefore do not consider these cases here.

The deterministic kinetic equations corresponding to the reactions given above are presented in the Supplemental Material [24], along with the analysis methods to determine the regions of bistability.

B. Promoter initiation dynamics

To test the effects of different RNA production dynamics, we employ two extra models of initiation. We characterize the amount of noise that these alternate RNA initiation models will produce in the RNA time series by the coefficient of variation (η, defined as the variance over the squared mean) of the distribution of time intervals between RNA production events. Except for very narrow, near-deterministic distributions, which is not the case here, the η^2 of this distribution captures the

TABLE I. Model parameters, values, and sources.

Parameter	Meaning	Value	Source
θ	Mean mRNA numbers	10^{-3}–1	Reference [20]
R	TF repression strength		
λ	srRNA repression strength		
α_m	mRNA production rate	$\theta\beta_m$ s^{-1}	See Methods
α_s	srRNA production rate	$\lambda\alpha_m$ s^{-1}	See Methods
β_m	mRNA degradation rate	600^{-1} s^{-1}	Reference [34]
β_s	srRNA degradation rate	3000^{-1} s^{-1}	Reference [41]
γ	mRNA-srRNA binding rate	$0.1\theta^{-1}$ s^{-1}	Reference [42]
α_p	Protein production rate	$B\beta_m$ s^{-1}	Set to match B
B	Protein burst size per mRNA	4.2	Reference [43]
β_p	Protein degradation rate	$36\,000^{-1}$ s^{-1}	References [35,36]
k_u	Unrepression rate	25^{-1} s^{-1}	Reference [44]
k_r	Repression rate	$k_{\text{unrep}}K_d^{-1}$ s^{-1}	Set to match K_d
K_d	TF-promoter dissociation constant	$\alpha_m B\beta_p^{-1}R^{-1}$	See Methods

contribution of the initiation dynamics to the fluctuations in the numbers of RNA and protein molecules over time [21].

The default reactions modeling RNA production are reactions (1) and (5). These result in an exponential distribution of time intervals between RNA production intervals, and thus have a η^2 of 1. Since this distribution produces a Poisson-distributed number of production events in a fixed time window, this initiation dynamics is termed Poissonian. Noisier-than-Poissonian production kinetics are achieved by a promoter that can randomly transition between an OFF and an ON state, and which only allows transcription when ON [19], producing bursts of RNA production. The reactions modeling this promoter are depicted in Fig. 1(b), and are as follows, where x is replaced by m or s when replacing reactions (1) or (5), respectively:

$$\text{Pro}_x^{\text{ON}} \xrightarrow{k_{\text{OFF}}} \text{Pro}_x^{\text{OFF}}, \tag{10}$$

$$\text{Pro}_x^{\text{OFF}} \xrightarrow{k_{\text{ON}}} \text{Pro}_x^{\text{ON}}, \tag{11}$$

$$\text{Pro}_x + \text{Pro}_x^{\text{ON}} \xrightarrow{k_t} \text{Pro}_x + \text{Pro}_x^{\text{ON}} + R_x. \tag{12}$$

Here, reaction (12) should not be confused for a bimolecular reaction. The notation only implies that the promoter must be ON and unrepressed for transcription to occur. We assume that bursts take a very short amount of time compared to the interburst time (i.e., $k_{\text{ON}} \ll k_{\text{OFF}}$), and thus set k_{OFF} to 1 s^{-1}. It can be shown (see Supplemental Material [24]) that reactions (10)–(12) produce a η^2 of $2S + 1$, where $S = k_t/k_{\text{OFF}}$ is the mean number of RNA molecules produced in each burst. To obtain a specific η^2 in Fig. 5(a), we therefore set $k_t = (\eta^2 - 1)/2$, and $k_{\text{ON}} = \alpha_x/S$ to match the mean production rate.

Sub-Poissonian dynamics is achieved with a promoter model that requires a series of Poissonian steps to be completed before an RNA is produced [26,27]. The reactions modeling this promoter dynamics are depicted in Fig. 1(c), and are as follows, where $N > 1$ is the total number of steps involved, $1 < n < N$, and x is replaced by m or s when replacing reactions (1) or (5), respectively:

$$\text{Pro}_x \xrightarrow{k_1} \text{Pro}_x^1, \tag{13}$$

$$\text{Pro}_x^{n-1} \xrightarrow{k_n} \text{Pro}_x^n, \tag{14}$$

$$\text{Pro}_x^{N-1} \xrightarrow{k_N} \text{Pro}_x + R_x. \tag{15}$$

It can be shown (see Supplemental Material [24]) that reactions (13)–(15) produce a η^2 of $1/N$. To obtain a specific η^2 in Fig. 5(a), we therefore set $N = 1/\eta^2$, and $k_i = N\alpha_x$ for $1 \leqslant i \leqslant N$ to match the mean production rate.

C. Characterization of noisy attractors

Stable states do not technically exist in the stochastic model above, since the probability that the system will leave any state after reaching it approaches 1 as time goes to infinity. We therefore use the term "noisy attractor" to refer to a set of microstates from which the system is unlikely to leave for a physiologically relevant time frame [28]. These noisy attractors correspond roughly, but not always, to the stable states found in the corresponding, deterministic model. For example, unstable steady states of the deterministic model will vanish in the stochastic model while stable steady states either remain the same or can vanish or settle around different mean molecule concentrations.

Since the system is not symmetric as in a toggle switch of two mutually repressing TF-coding genes, it is not immediately clear how to group the microstates of the system into noisy attractors. Here, the categorization was performed by examining the overall joint distribution of TF and srRNA populations for each value of θ and selecting a threshold in this plane that separated the two modes. States for which $P - 10R_s - 10\theta > 0$ were classified as part of the TF-high noisy attractor, while other microstates were categorized as part of the srRNA-high noisy attractor.

The stability of a noisy attractor is defined as the mean time that the system will remain in that region of the state space before stochastically leaving it (and in this case, traveling to the other noisy attractor). For both noisy attractors, this quantity was measured by initializing a simulation with RNA and/or

protein populations set to the mean amount that would be produced with no repression (i.e., $R_m = \theta$ and $P = \alpha_m B\beta_p^{-1}$ for TF-high and $R_s = \alpha_s/\beta_s$ for srRNA-high) and simulating until it switched to the other noisy attractor, sampling every hour, limited to 1 month of simulation time. Simulations were conducted in SGNS2 [29], a stochastic molecular dynamics simulator based on the stochastic simulation algorithm [30].

III. RESULTS

The bistable regions of the parameter space of the deterministic version of the SMDFL have been studied previously [7]. The regions of bistability found in the deterministic solution are recovered in the high-copy-number limit of the present model (Fig. S1 in Supplemental Material [24]), i.e., in the high-θ limit. Since θ was chosen to represent the mean RNA numbers of the unrepressed TF-encoding gene, we can use genome-wide measurements in cell populations of *Escherichia coli* to place it within a realistic range, measured to be $\sim 10^{-3}$–1 [20].

A. Robust bistability

We first study what TF and srRNA repression strengths (parameters R and λ, respectively) are required to achieve robust bistability in the stochastic model with $\theta = 1$, at the higher end of the realistic range. We define "robust bistability" as when the system can remain in either noisy attractor for at least 1 month of simulation time, on average. Results are shown in Fig. 2(a). In this case, robust bistability is achieved when $\lambda > 2.75$ and R is sufficiently strong for the chosen λ. This is shown in Fig. 2(b), where the TF population from two independent runs holds its initial state (high or low) for the duration of the simulation. Meanwhile, Fig. 2(d) shows monostability, where the system is unable to stay in the srRNA-high, TF-low noisy attractor due to insufficient λ, despite lying within the parameter region of deterministic bistability. Figure 2(c) shows the classic stochastic toggle switch behavior where the switch stochastically jumps between the two noisy attractors.

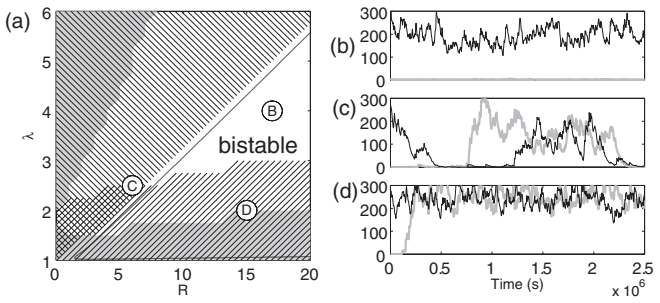

FIG. 2. (a) Bifurcation diagram with λ and R as control parameters and $\theta = 1$. Hatched areas indicate where a noisy attractor is not robustly stable (i.e., stable for less than 90% of 1 month of simulation time, on average). Upwards and downwards hatching indicates the srRNA-high and TF-high noisy attractors are unstable, respectively. Shaded areas indicate that the unstable noisy attractor is less stable than 5% of 1 month of simulation time (i.e., the switch is monostable or unstable). This diagram and all subsequent ones are from 500 runs per tested parameter pair and initial state. The solid line indicates the extent of the region where the deterministic model is bistable (see Supplemental Material [24]). Example time series of TF populations alone are shown from two independent simulations with (b) $R = 17$, $\lambda = 4$ (robustly bistable), (c) $R = 6$, $\lambda = 2.5$ (weak bistability), and (d) $R = 15$, $\lambda = 2$ (monostable), with initial conditions set to start in the TF-high (black line) and in the srRNA-high, TF-low (gray line) noisy attractors. Note that in (b), the gray line remains very low for the duration of the simulation.

The region of robust bistability appears to be a subset of the region of deterministic bistability in Fig. 2(a). Interestingly, outside the region of deterministic bistability, it is possible for one or both of the noisy attractors to be only transiently stable. That is, the system remains in a noisy attractor for 5%–90% of 1 month of simulation time. When both noisy attractors are only transiently stable, the switch stochastically transitions unbiasedly between them [double-hatched region in Fig. 2(a)].

The highest value of R shown, 20, corresponds to a dissociation constant between the promoter and the TF of approximately $K_d = \theta\beta_m B\beta_p^{-1}R^{-1} = 12$ molecules, which is within realistic ranges for TF-promoter interactions [31]. Thus, the TF repression strength required to achieve robust bistability is within realistic bounds. We are not aware of measurements of srRNA production rates. Nevertheless, using transcription rates of protein-coding genes [20] as a guide, the values of λ required to achieve robust stability are high, since the high value of θ already places the mRNA production rate at the upper limit of the range observed in *E. coli* [20]. Thus, we next study how the bifurcation diagram changes for lower θ.

B. Low copy numbers

Low-copy-number effects, i.e., when θ is lowered, are expected to significantly affect the stability of the noisy attractors of the switch. This is shown in Fig. 3, as θ is lowered from 1 to 0.5, 0.2, and finally 0.1. Robust bistability (i.e., existence of two distinct noisy attractors) is observable within realistic ranges for a limited range for $\theta = 0.5$. The likely cause for this is that srRNA-based repression is based on the interaction between two species with few copies in the cell at any given time. Consistent with this explanation, the strength of TF repression required to stabilize the TF-high noisy attractor is largely unchanged from the $\theta = 1$ case.

For $\theta = 0.2$ and $\theta = 0.1$, robust bistability is lost for the same parameter range. Worse, the same value of R corresponds to increasing repression strength as θ is decreased, and with $R = 20$ and $\theta = 0.1$ this corresponds to a TF-promoter dissociation constant of less than $\sim$ two molecules, which is extreme but realizable [32]. The region where both noisy attractors are

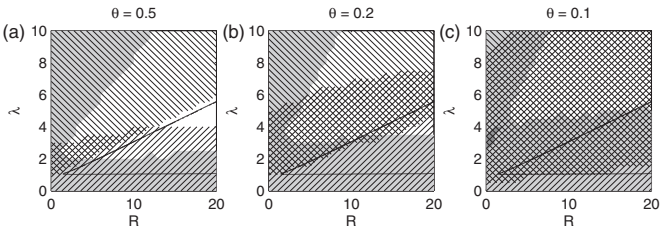

FIG. 3. Bifurcation diagram with λ and R as control parameters, with (a) $\theta = 0.5$, (b) $\theta = 0.2$, (c) $\theta = 0.1$.

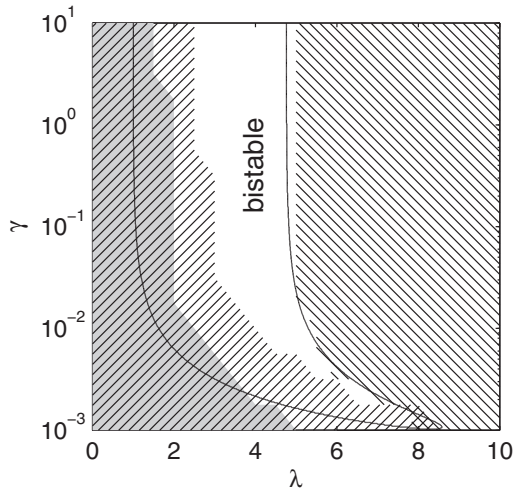

FIG. 4. Bifurcation diagram using γ and λ as control parameters, with $\theta = 1$ and $R = 17$.

stable on an intermediate time scale grows as θ is reduced, and begins to cover most of the tested parameter space. Thus, short-term bistability remains possible in this regime.

C. mRNA-srRNA binding

One parameter for which we could not find measurements is γ, which was set following a previous model of srRNA regulation. This parameter controls the time it will take for an mRNA to bind to an srRNA, and therefore affects the effectiveness of srRNA repression. To understand how this parameter can affect the switch, we generated the bifurcation diagram of the switch using λ and γ as control parameters, shown in Fig. 4. Above a certain critical value, here $\sim$0.01 s^{-1} per mRNA-srRNA pair, the dynamics does not change significantly. Below this value, the region of bistability shrinks rapidly to a point where small changes in γ can move the switch from monostable TF-high to monostable srRNA-high.

We note that γ scales inversely with θ. This scaling allows the stochastic model to converge to the deterministic solution in the high-θ limit. We tested whether the changes observed in Fig. 3 resulted from this scaling. Setting γ to 0.1 (Fig. S2, Supplemental Material [24]), we found no appreciable change.

D. Promoter kinetics

Since regulation by srRNA has been shown to have nontrivial noise characteristics [4], it is of interest to study how a network involving srRNA interactions behaves with different noise properties. To this end, we varied the level of noise introduced by transcription initiation and observed how it affects the stability of the switch, starting from a parameter set where robust bistability is observed when both promoters are Poissonian ($\lambda = 4$ and $R = 17$). The level of noise in the production of an RNA species was adjusted by replacing the appropriate RNA production reaction [reaction (1) or (5)] with a set of reactions producing a distribution of intervals between production events with a given η^2 [reactions (10)–(12) for $\eta^2 > 1$ or reactions (13)–(15) for $\eta^2 < 1$; see Methods]. The results are shown in Fig. 5(a).

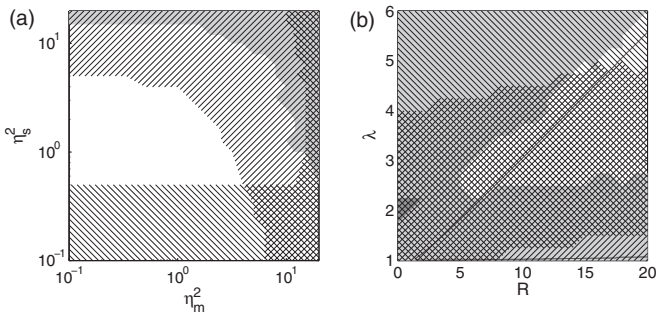

FIG. 5. (a) Bifurcation diagram with different promoter kinetics. Control parameters are the η^2 (variance over the squared mean) of the time interval distribution between transcription initiations for the srRNA production (η_s^2) and for the TF production (η_m^2), assuming no regulation. These were modified by replacing reactions (1) or (5), or both with reaction sets (10)–(12) or (13)–(15) to obtain a given η^2 for both mRNA and srRNA production intervals (see Methods). For reference, the least noisy interval distribution has $N = 10$ steps, while the most noisy has a burst size of $S = 9.5$. $\theta = 1$, $\lambda = 4$, $R = 17$. (b) Bifurcation diagram as in Fig. 3(b), with $\theta = 0.2$, and a four-step promoter for srRNA.

When either promoter is bursty, the srRNA-high noisy attractor loses stability. This is expected, since srRNA regulation involves interaction between two RNA species, which are both in low copy number. Consistent with this, the noise in srRNA production (η_s^2) has the strongest overall effect on the stability, determining whether it is bistable or monostable in either noisy attractor. Since it is monostable in the low-noise srRNA production region, it appears that this allows it to repress its target more consistently. Given the loss of bistability in the low-θ region of the parameter space [Figs. 3(a)–3(c)], it is plausible that this increase in regulation strength with more deterministic production might allow the switch to operate more effectively for low θ. We therefore repeated Fig. 3(c) with four-step, sub-Poissonian srRNA production, shown in Fig. 5(b). This change was not sufficient to restore robust bistability in the parameter range tested. Instead, although the λ required to stabilize the srRNA-high noisy attractor has decreased, this change came at the cost of the stability of the TF-high noisy attractor. That is, the R required to stabilize the TF-high noisy attractor is considerably greater. Note that no deterministic region of bistability is displayed in Fig. 5(a), since no parameters affecting deterministic bistability were varied in this figure.

E. Asymmetric switching

Robust bistability is achievable in noncooperative TF-based toggle switches as well [25]. Under what circumstances then would an srRNA-mediated switch be preferable to use in a real genetic circuit rather than a purely TF-mediated switch? One difference between the two motifs is that one of the regulatory molecules (the srRNA) has a much smaller half-life than most natural proteins, despite its extended lifetime due to the binding of Hfq [33] in comparison to mRNA [34]. This allows its level to decrease more quickly in response to regulation. We therefore expect that the switch is able to change from the srRNA-high noisy attractor to the TF-high noisy attractor

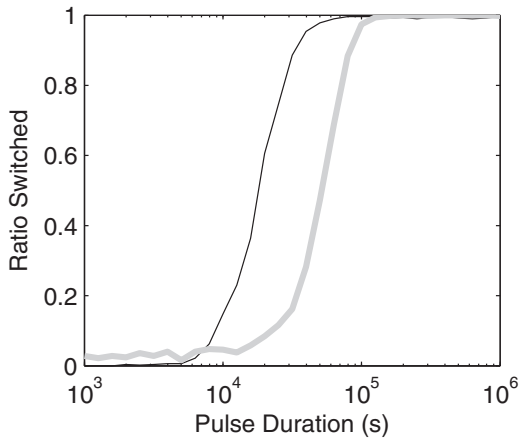

FIG. 6. Fraction of SMDFL switches that changed noisy attractor and remained in the new one after an input pulse of varying duration. The simulation was started in either the srRNA-high (black line) or the TF-high noisy attractor (thick gray line), with $\theta = 1$, $R = 15$, and $\lambda = 4$. The simulation was first run for 100 h, after which an input pulse of the given duration was applied, where R or λ was scaled by 0.2, to push the switch into the opposite noisy attractor. After the pulse, the simulation was run for another 100 h to allow the switch to settle into its new noisy attractor, and the final state was measured. Data are from 500 simulations for each tested pulse duration.

much faster than vice versa. To test this, we simulated the switch, starting in one of the two noisy attractors, in a robustly bistable region of the parameter space ($R = 15$, $\lambda = 4$, $\theta = 1$) for 100 h, and applied an input pulse of varying durations. This pulse moved the system into a region of the parameter space which is monostable in the other noisy attractor by scaling R or λ by $1/5$. The switch was then simulated for another 100 h and the final state was recorded.

The fraction of times the switch was found in the other noisy attractor at that stage is shown in Fig. 6. From the figure, the switch displays a strong asymmetry in the duration of the input pulse required to switch noisy attractor. Specifically, half of srRNA-high simulations ended in the TF-high noisy attractor after applying a pulse of 15 000 s, while switches in the TF-high attractor take a much longer input pulse of 50 000 s for half to change noisy attractors.

IV. CONCLUSIONS AND DISCUSSION

Using a stochastic model of the SMDFL with most parameters taken from the literature, we showed that, within realistic parameter ranges, this model can exhibit robust bistability. That is, the stochastic fluctuations of RNA and protein numbers cannot, on average, cause the switch to change noisy attractor within 1 month of simulation time. Reducing the mean RNA and protein numbers (i.e., increasing the finite-size effects) limited the regions of robust bistability, owing to the inability of the srRNA to reliably repress its target at such low mean levels. Realistically realizable regions of long-term bistability exist down to $\theta = 0.5$, despite the absence of cooperative repression by the TF. Below this, robust bistability is lost for realistic repression strengths. Similarly, for highly noisy srRNA production and for noisy mRNA production, the srRNA loses effectiveness, with the srRNA production variability having the largest impact. Lower levels of noise in srRNA production increase the effectiveness of the srRNA regulation, but decrease the stability of the TF-high noisy attractor, and thus cannot be used to compensate for low-copy-number effects to regain bistability in the low-RNA parameter range. Thus, such switches must operate at the higher end of the mean RNA number spectrum in order to function reliably, or must have some additional machinery to strengthen the regulation such as cooperative repression by the TFs.

One of the parameters for which we could not find measurements in the literature is γ, which controls the mRNA-srRNA binding rate. Examining the dependence of the dynamics on this parameter reveals that there is a point, here $\sim 0.01\theta^{-1}$ s^{-1} per mRNA-srRNA pair, beyond which further increases do not change the dynamics of the switch. Below this point, the bistability of the switch is sensitive to changes in γ. This parameter controls the rate of a bimolecular reaction, and is therefore likely to be diffusion limited, and will change with, for example, temperature. Having a slow binding rate and placing the switch in the lower-right portion of the parameter space shown in Fig. 4 might therefore be a way to create a temperature-dependent switch, without the need for a specific sensing apparatus.

By applying input pulses of varying time length to determine how quickly the switch can change to another noisy attractor under external control, we determined that the change from the srRNA-high noisy attractor to the TF-high noisy attractor is considerably faster than the reverse, due to the higher degradation rate of the srRNA. This asymmetry allows rapid changes from one noisy attractor to the other based on a single, short input, but requires a much longer, sustained input to change the other way. Most proteins have much longer half-lives [35,36], making this hard to achieve in switches relying on TFs alone, though it could be accomplished by active degradation of the proteins [37], which thus requires a larger number of interactive players in the system (and, most likely, additional energy expenditure).

We note that the present model does not include the effects of cellular growth and division, which act as an increased degradation rate of all cellular components. This will affect proteins more than RNAs since they have a longer mean lifetime. This should cause the asymmetry in switching times to decrease, but remain, in fast-growing bacterial populations under optimal growth conditions. However, in natural environments, cell populations are not commonly under optimal conditions meaning that the mean division rates are much slower. It is also worthwhile to note that, similar to results from measurements in live cells, our results are expected to depend, to some extent, on the values of some of the parameters not varied in the present study. Our choice of parameters to vary was based on our observations of which were more prone to cause behavior modifications. Nevertheless, future studies may provide additional insight into the currently unknown relevance of some of the untested parameters. Another interesting study would be to investigate how the kinetics of the model changes with cell growth phase. Finally, we note that, when considering the effects of cell division, we also expect that it is necessary to account for the effects of asymmetries in the partitioning of cellular components,

including RNA and proteins, as well as for the effects of cellular aging [38].

Asymmetry in the switching between noisy attractors may be of use, particularly given the physiologically relevant difference in the duration of the pulses required to switch between the noisy attractors. For example, the iron storage regulator Fur and srRNA RyhB are arranged in the SMDFL motif in several bacterial species [8]. Since Fur only represses RyhB transcription when Fe^{2+} is present, we predict that the transition from the RyhB-high state (with no iron storage genes active) to the Fur-high state will require a relatively short time in an iron-rich environment. Conversely, it will take much longer to disable the iron storage genes when transitioning to an iron-deficient environment.

Finally, we note that the model employed here makes a number of simplifying assumptions, which may limit the applicability of the results. First, transcription and translation are assumed to take no time. These processes introduce delays, which can be non-negligible in the dynamics of a switch [39]. These delays are expected to be longer in eukaryotes, where several additional processes such as pre-mRNA processing and nuclear export must take place to produce the TFs and repress the target [40]. However, these delays have been shown to generally have smaller effects on the dynamics of a switch than the delay caused by the open complex formation at the promoter [39], which was modeled here in the less noisy promoter model. We thus believe that the results are reasonably applicable to eukaryotes and to prokaryotes in stationary phase.

ACKNOWLEDGMENTS

Work was supported by TUT President's Doctoral Programme (J.L.-P.), and Academy of Finland (A.S.R.). The funders had no role in study design, data collection and analysis, decision to publish, or preparation of the manuscript.

[1] A. S. Flynt and E. C. Lai, Nat. Rev. Genet. **9**, 831 (2008).
[2] G. Storz, S. Altuvia, and K. M. Wassarman, Annu. Rev. Biochem. **74**, 199 (2005).
[3] S. Gottesman, Trends Genet. **21**, 399 (2005).
[4] E. Levine, M. Huang, Y. Huang, T. Kuhlman, H. Shi, Z. Zhang, and T. Hwa [Proc. Natl. Acad. Sci. USA (to be published)].
[5] S. Mukherji, M. S. Ebert, G. X. Y. Zheng, J. S. Tsang, P. A. Sharp, and A. van Oudenaarden, Nat. Genet. **43**, 854 (2011).
[6] Y. Shimoni, G. Friedlander, G. Hetzroni, G. Niv, S. Altuvia, O. Biham, and H. Margalit, Mol. Syst. Biol. **3**, 138 (2007).
[7] P. Zhou, S. Cai, Z. Liu, and R. Wang, Phys. Rev. E **85**, 041916 (2012).
[8] B. Večerek, I. Moll, and U. Bläsi, EMBO J. **26**, 965 (2007).
[9] F. Fazi, A. Rosa, A. Fatica, V. Gelmetti, M. L. De Marchis, C. Nervi, and I. Bozzoni, Cell **123**, 819 (2005).
[10] X. Li and R. W. Carthew, Cell **123**, 1267 (2005).
[11] C. P. Bracken, P. A. Gregory, N. Kolesnikoff, A. G. Bert, J. Wang, M. F. Shannon, and G. J. Goodall, Cancer Res. **68**, 7846 (2008).
[12] A. H. Juan, R. M. Kumar, J. G. Marx, R. A. Young, and V. Sartorelli, Mol. Cell **36**, 61 (2009).
[13] A. Arkin, J. Ross, and H. H. McAdams, Genetics **149**, 1633 (1998).
[14] U. Alon, Nat. Rev. Genet. **8**, 450 (2007).
[15] L. Wang, B. L. Walker, S. Iannaccone, D. Bhatt, P. J. Kennedy, and W. T. Tse, Proc. Natl. Acad. Sci. USA **106**, 6638 (2009).
[16] S. Huang, Y.-P. Guo, G. May, and T. Enver, Dev. Biol. **305**, 695 (2007).
[17] M. Acar, J. T. Mettetal, and A. van Oudenaarden, Nat. Genet. **40**, 471 (2008).
[18] J. Elf, J. Paulsson, O. G. Berg, and M. Ehrenberg, Biophys. J. **84**, 154 (2003).
[19] I. Golding, J. Paulsson, S. M. Zawilski, and E. C. Cox, Cell **123**, 1025 (2005).
[20] Y. Taniguchi, P. J. Choi, G.-W. Li, H. Chen, M. Babu, J. Hearn, A. Emili, and X. S. Xie, Science (NY) **329**, 533 (2010).
[21] A.-B. Muthukrishnan, M. Kandhavelu, J. Lloyd-Price, F. Kudasov, S. Chowdhury, O. Yli-Harja, and A. S. Ribeiro, Nucleic Acids Res. **40**, 8472 (2012).
[22] M. Kandhavelu, J. Lloyd-Price, A. Gupta, A.-B. Muthukrishnan, O. Yli-Harja, and A. S. Ribeiro, FEBS Lett. **586**, 3870 (2012).
[23] Y. Hao, L. Xu, and H. Shi, J. Mol. Biol. **406**, 195 (2011).
[24] See Supplemental Material at http://link.aps.org/supplemental/10.1103/PhysRevE.88.032714 for the analysis of the deterministic model, explanation of η^2 for the promoter kinetics, and supplemental figures.
[25] A. Lipshtat, A. Loinger, N. Q. Balaban, and O. Biham, Phys. Rev. Lett. **96**, 188101 (2006).
[26] H. Buc and W. R. McClure, Biochemistry **24**, 2712 (1985).
[27] M. Kandhavelu, H. Mannerström, A. Gupta, A. Häkkinen, J. Lloyd-Price, O. Yli-Harja, and A. S. Ribeiro, BMC Syst. Biol. **5**, 149 (2011).
[28] A. S. Ribeiro and S. A. Kauffman, J. Theor. Biol. **247**, 743 (2007).
[29] J. Lloyd-Price, A. Gupta, and A. S. Ribeiro, Bioinformatics **28**, 3004 (2012).
[30] D. T. Gillespie, J. Phys. Chem. **81**, 2340 (1977).
[31] M. Merika and S. H. Orkin, Mol. Cell. Biol. **13**, 3999 (1993).
[32] A. K. Vershon, S. Liao, W. R. McClure, and R. T. Sauer, J. Mol. Biol. **195**, 311 (1987).
[33] T. Møller, T. Franch, P. Højrup, D. R. Keene, H. P. Bächinger, R. G. Brennan, and P. Valentin-Hansen, Mol. Cell **9**, 23 (2002).
[34] J. A. Bernstein, A. B. Khodursky, S. Lin-Chao, and S. N. Cohen, Proc. Natl. Acad. Sci. USA **99**, 9697 (2002).
[35] K. L. Larrabee, J. O. Phillips, G. J. Williams, and A. R. Larrabee, J. Biol. Chem. **255**, 4125 (1980).
[36] R. D. Mosteller, R. V. Goldstein, and K. R. Nishimoto, J. Biol. Chem. **255**, 2524 (1980).
[37] S. Göttesman, Annu. Rev. Genet. **30**, 465 (1996).
[38] E. J. Stewart, R. Madden, G. Paul, and F. Taddei, PLoS Biol. **3**, e45 (2005).
[39] A. S. Ribeiro, A. Häkkinen, H. Mannerström, J. Lloyd-Price, and O. Yli-Harja, Phys. Rev. E **81**, 011912 (2010).

[40] M. J. Moore and N. J. Proudfoot, Cell **136**, 688 (2009).
[41] I. Moll, RNA **9**, 1308 (2003).
[42] E. Levine, Z. Zhang, T. Kuhlman, and T. Hwa, PLoS Biol. **5**, e229 (2007).
[43] J. Yu, J. Xiao, X. Ren, K. Lao, and X. S. Xie, Science (NY) **311**, 1600 (2006).
[44] M. Dunaway, J. S. Olson, J. M. Rosenberg, O. B. Kallai, R. E. Dickerson, and K. S. Matthews, J. Biol. Chem. **255**, 10115 (1980).